

## Full wave propagation modelling in view to integrated ICRH wave coupling/RF sheaths modelling

Jonathan Jacquot<sup>\*</sup>, Volodymyr Bobkov, Laurent Colas, Stéphane Heuraux, Alena Křivská, Lingfeng Lu, Jean-Marie Noterdaeme, Tore Supra Team, and ASDEX Upgrade Team

Citation: [AIP Conference Proceedings](#) **1689**, 050008 (2015); doi: 10.1063/1.4936496

View online: <http://dx.doi.org/10.1063/1.4936496>

View Table of Contents: <http://aip.scitation.org/toc/apc/1689/1>

Published by the [American Institute of Physics](#)

---

---

# Full Wave Propagation Modelling in View to Integrated ICRH Wave Coupling/RF Sheaths Modelling

Jonathan Jacquot<sup>1,a)</sup>, Volodymyr Bobkov<sup>1</sup>, Laurent Colas<sup>2</sup>, Stéphane Heuraux<sup>3</sup>, Alena Křivská<sup>4</sup>, Lingfeng Lu<sup>2</sup>, Jean-Marie Noterdaeme<sup>1,5</sup>, Tore Supra Team and ASDEX Upgrade Team

<sup>1</sup>Max-Planck Institut für Plasmaphysik, Garching, Germany

<sup>2</sup>CEA, IRFM, F-13108 Saint-Paul-Lez-Durance, France

<sup>3</sup>Institut Jean Lamour UMR 7198 CNRS-Université de Lorraine, Nancy, France

<sup>4</sup>LPP-ERM/KMS, Royal Military Academy, Brussels, Belgium

<sup>5</sup>Department of Applied Physics, Ghent University, Belgium

<sup>a)</sup>Corresponding author: jonathan.jacquot@ipp.mpg.de

**Abstract.** RF sheaths rectification can be the reason for operational limits for Ion Cyclotron Range of Frequencies (ICRF) heating systems via impurity production or excessive heat loads. To simulate this process in realistic geometry, the Self-consistent Sheaths and Waves for Ion Cyclotron Heating (SSWICH) code is a minimal set of coupled equations that computes self-consistently wave propagation and DC plasma biasing. The present version of its wave propagation module only deals with the Slow Wave assumed to be the source of RF sheath oscillations. However the ICRF power coupling to the plasma is due to the fast wave (FW). This paper proposes to replace this one wave equation module by a full wave module in either 2D or 3D as a first step towards integrated modelling of RF sheaths and wave coupling. Since the FW is propagative in the main plasma, Perfectly Matched Layers (PMLs) adapted for plasmas were implemented at the inner side of the simulation domain to absorb outgoing waves and tested numerically with tilted  $B_0$  in Cartesian geometry, by either rotating the cold magnetized plasma dielectric tensors in 2D or rotating the coordinate vector basis in 3D. The PML was further formulated in cylindrical coordinates to account for the toroidal curvature of the plasma. Toroidal curvature itself does not seem to change much the coupling. A detailed 3D geometrical description of Tore Supra and ASDEX Upgrade (AUG) antennas was included in the coupling code. The full antenna structure was introduced, since its toroidal symmetry with respect to the septum plane is broken (FS bars, toroidal phasing, non-symmetrical structure). Reliable convergence has been obtained with the density profile up to the leading edge of antenna limiters. Parallel electric field maps have been obtained as an input for the present version of SSWICH.

## CONTEXT AND GOALS

RF sheaths rectification can be the reason for operational limits for Ion Cyclotron Range of Frequencies (ICRF) heating systems via impurity production or excessive heat loads. The present version of the SSWICH code [1] that aims at modelling in a self-consistent manner RF sheaths only deals with the slow wave while power coupling to the plasma is due to the fast wave. This contribution proposes a first step towards full wave integrated modelling of RF sheaths and wave coupling. RF sheaths aspects are not implemented but should be compatible with this framework. One of the essential pieces for the ICRF wave modelling in the edge plasma (i.e. simulation domain) is to be able to deal with outgoing propagative waves without reflection since no inherent efficient absorption mechanism exists in the edge for these waves. For that purpose, Perfectly Matched Layers (PMLs) [2] for magnetized plasmas are implemented. Another essential piece is an accurate description of the antenna geometry and the plasma it is immersed into, considering the cold plasma approximation. This paper briefly summarizes the PML technique before applying it to ICRF antennas modelling in magnetized plasmas in 2D and in 3D with different coordinates systems.

## PERFECTLY MATCHED LAYER THEORY FOR TOROIDALLY CURVED PLASMAS

PMLs are nowadays a common tool to emulate radiating boundary conditions at infinity, commonly used in modelling classical dielectric material with open boundaries domain. However they are still relatively new in fusion plasmas [3]. The PML can be interpreted as an artificial anisotropic absorbing medium, where the standard equations of

electrodynamics can be applied in their usual form. A complete formulation of general closed-form PML in bi-anisotropic and dispersive media can be found in [4]. The case treated here considers the constitutive relations  $\mathbf{D} = \bar{\bar{\epsilon}}\mathbf{E}$  and  $\mathbf{B} = \bar{\bar{\mu}}\mathbf{H}$ , where for the sake of generality the dielectric tensor  $\bar{\bar{\epsilon}}$  and magnetic permeability tensor  $\bar{\bar{\mu}}$  are full.

The standard system of Maxwell's equations in a medium is replaced by a modified system of Maxwell's equations over the whole computation domain being constituted of the medium, the PMLs layers and radiation conditions at the boundaries of the main simulation domain. Following [4], the space coordinates are transformed by an analytic continuation to a complex variable spatial domain written with stretching functions deforming the space. The solution of the problem in 3D geometry should remain unchanged in the main computational domain where the stretched coordinates coincide with the normal ones. The analytic continuation is formally expressed by the following transformation:  $u \rightarrow t_u = \int_0^u S_u(u') du'$ , where  $S_u = S'_u + iS''_u$  are the complex stretching functions and  $u$  stands for any of the space coordinates:  $x, y, z$  in Cartesian coordinates or  $r, \varphi, Z$  in cylindrical coordinates.  $S_u$  can be chosen with great flexibility, but should depend exclusively on coordinate  $u$  (i.e.  $S_u = S_u(u)$ ). They define the stretching tensor and  $\bar{\bar{S}} = \text{diag}_{i=1}^3 S_{u_i}$ . In cylindrical coordinates, the toroidal direction denoted by  $z$  in cartesian coordinates is replaced with  $\varphi$ . It allows the toroidal curvature to be included in the model. It also imposes a modification in the corresponding stretching function:  $S_z \rightarrow S_\varphi t_r / r$ . In the end, the standard equations of electrodynamics are applied. However, the original RF fields  $\mathbf{E}$  and  $\mathbf{H}$  are replaced respectively by artificial RF fields  $\bar{\bar{S}}\mathbf{E}$  and  $\bar{\bar{S}}\mathbf{H}$ . The original and artificial RF fields coincide inside the main simulation domain, where the stretching tensor is the identity tensor ( $\bar{\bar{S}} = \bar{\bar{I}}$ ). The original tensors  $\bar{\bar{\epsilon}}$  and  $\bar{\bar{\mu}}$  are replaced respectively with the artificial tensors  $\bar{\bar{\epsilon}}_{PML} = \bar{\bar{\Lambda}} \cdot \bar{\bar{\epsilon}} \cdot \bar{\bar{S}}^{-1}$  and  $\bar{\bar{\mu}}_{PML} = \bar{\bar{\Lambda}} \cdot \bar{\bar{\mu}} \cdot \bar{\bar{S}}^{-1}$  where  $\bar{\bar{\Lambda}} = \det(\bar{\bar{S}}) \bar{\bar{S}}^{-1}$ .

## SIMULATION RESULTS

Since 2D models are easier to create and handle, 2D models were first created in Cartesian and in cylindrical coordinates for a generic and parametrized 2 or 3 straps antenna. The feeding system is however not realistic nor self-consistent since it is localized in the third out of plane direction. Instead surface current densities are enforced on each edges of the strap. A convex parabolic current density profile is considered on the front edge (in regard to the plasma) and the back edge on the contrary to the constant current densities in [3]. Linear densities are imposed on the side edges. The straps can also be rotated through its center to be aligned with the curvature.

Simulations have shown that the radiated electric field pattern (see Figure 1a) is similar in both coordinates systems. The coupled power vary by less than 10% when the toroidal curvature radius is changed. Most of it is due to the fact that the distance strap/FW R-cutoff is not constant anymore. Instead an average distance should be considered. A large curvature radius gives again what is expected in Cartesian coordinates. While it does not change much the coupling, the curvature can change significantly the amplitude of the near parallel electric field. Toroidal curvature could be important for the modelling of RF sheaths. Poloidal curvature associated with poloidal variation of the density in a 3D model is more likely to be significant for wave coupling efficiency.

Crossing the lower hybrid resonance (LH) layer is a significant hurdle as shown in [6]. Different methods exist to avoid it. A very sharp transition from vacuum to plasma density above the LH resonance was considered in [3]. Other solutions can be considered:

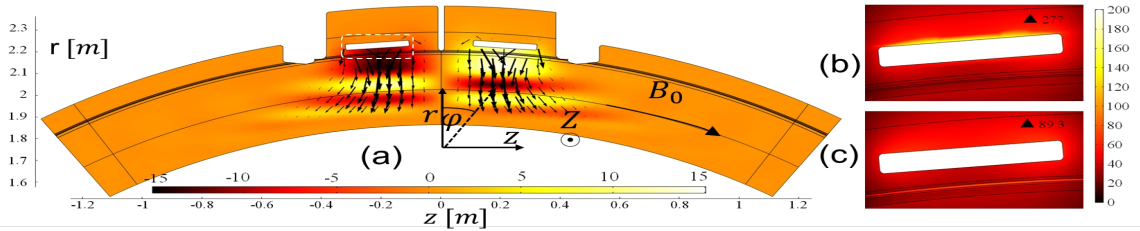


**FIGURE 1.** a) 2D Map of the real part of the poloidal electric field for a generic 2 straps antenna in cylindrical geometry on a 30° toroidal section on the torus and a plasma radial size of 15cm. The black arrows represent the Poynting vector. The axis  $r$  and  $z$  as well as the coordinate systems are shown. 2D map of the norm of the total electric field  $|E_{tot}|$  around the left strap for b) a finite density above the LH resonance in the antenna and c) an imaginary frequency around the LH resonance layer. The maximum value of  $|E_{tot}|$  are written in black.

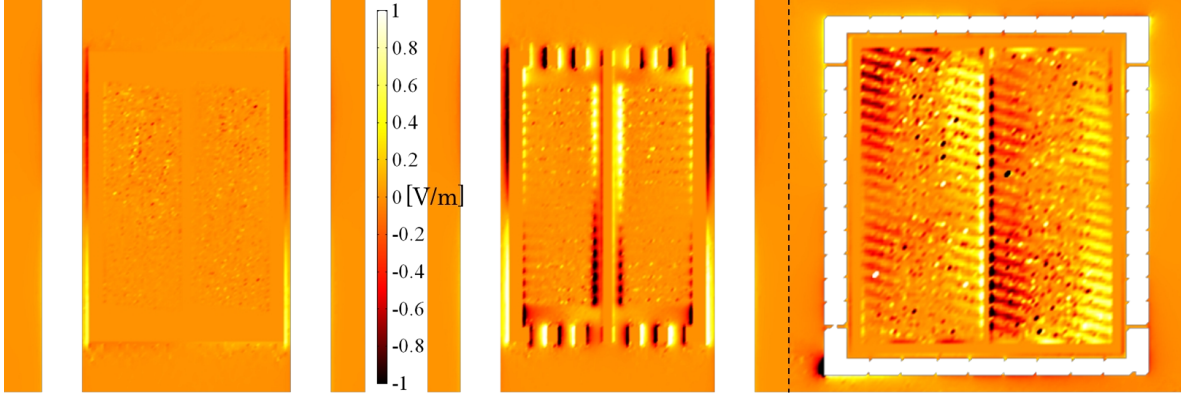


**FIGURE 2.** Antenna geometries included the model: 2 straps Tore Supra antenna with a) classical Faraday screen (FS), b) prototype FS [5], c) classical 2 straps AUG antenna with standard limiters, d) new 3 straps AUG antenna. Corresponding parallel electric field maps for 1V at each feeder at the FS position for the antenna geometries a-c. The magnetic field tilt is aligned with the FS bars in a')  $\theta = 7^\circ$ , b')  $\theta = 0^\circ$  and c')  $\theta = 15^\circ$ . The color scale for c' is the same as for fig. 3.

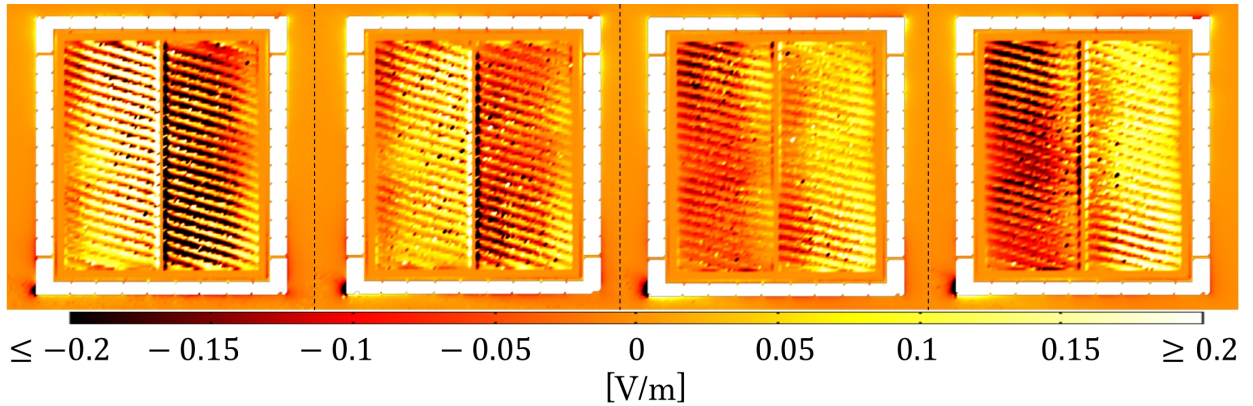


**FIGURE 3.** Parallel electric field maps for 1V at each feeder of antenna geometry 2c) during a scan of the magnetic field tilt: a)  $\theta = 7^\circ$ , b)  $\theta = 11^\circ$ , c)  $\theta = 19^\circ$  and d)  $\theta = 23^\circ$ . The FS screen bars are tilted by  $15^\circ$ .

1. Having a finite density above the resonance in the antenna by definition avoids the LH resonance (see Figure 1b)).
2. An imaginary frequency  $\nu_0$  can be added locally around the LH resonance layer to provide a damping mechanism (see Figure 1c). The antenna frequency  $f_0$  is thus replaced by  $f_0 + i\nu_0$  around the LH layer.

The first solution naturally solves the issue at the LH resonance at the expense of a finite density plasma on the strap itself. The amplitude and distribution of the electric field on the strap are modified compared to the fields with the strap located in vacuum. With the second solution, the strap is located in vacuum. The fields are higher in a thin region around the LH resonance but they stay reasonable by choosing accordingly  $\nu_0$ . During a scan of  $\nu_0$ , a minimum amplitude of the fields in the LH layer can be obtained. In this case with a pure deuterium plasma,  $f_0 = 38\text{MHz}$ , the local magnetic field  $B = 1.86\text{T}$ , the minimum amplitude is obtained for  $\nu_0 = 15\text{MHz}$ .

A first version of a 3D model was developed in [3]. It relied on many assumptions to simplify the antenna geometry, used symmetry properties and has a relatively low computational cost. The different sources of asymmetry were removed. The next phase consisted in progressively removing the symmetries and thus include the sources of asymmetry (tilted FS, asymmetric straps, asymmetric strap feeding, odd number of straps, tilted magnetic field). To that end, a half Tore Supra antenna was taken as the initial step. The sources of asymmetries were progressively included as well as a more detailed geometry (shaped limiters, FS bars, shark teeth in Figure 2b, limiter tiles on AUG antennas). That process, where the order of complexity is increased, can be summarized by a step by step transformation from a Tore Supra antenna to an AUG antenna. Presently 3D flat parametrized models exist for Tore Supra

(Figures 2a-b and AUG antennas (Figures 2c-d) without any curvature as well as hybrid geometries. The poloidal tilt of the magnetic field  $\theta$  is accounted for by rotating the cartesian vector basis frame with the Euler angles that keeps the natural form of the tensors and ease the PMLs implementation whose interface with the medium should always be normal to one direction. A first attempt at including curvature in 3D modelling has failed due to the difficulty to mesh objects with different curvatures. At the very least, a relevant model to study the influence of poloidal variation of the density must include a plasma curvature different from the antenna curvature. The convergence is not yet ensured when a finite density profile exists in the private region of the antenna due to probable issues with the mesh resolution. For this reason, the density is stopped at the leading edge of the antenna limiters.

Parallel (with respect to the magnetic field orientation) electric field maps for the antenna geometries, illustrated by Figures 2a'-c', have been obtained as an input for the present version of SSWICH [1]. For Tore Supra antennas, the field map is consistent with previous results [1] obtained with TOPICA [7] and with experiments [8]. The surface of the antenna is almost 4 times the one of Tore Supra antenna with finer geometrical details. This entailed a finer mesh whose resolution is limited by the available computational resources. For the AUG antennas, a higher level of meshing is needed. The transparency of the FS of the AUG has also been artificially increased by removing half the bars. The real gap between bars (smaller than one bar) could not be accurately meshed, preventing the capacitive fields generated between the straps and the antenna box to cross the FS typically seen in previous modelling attempt [9]. Some fields are also generated on the limiters frame with the maximum near the corners. A scan of  $\theta$ , illustrated by Figures 2c' and 3, show that the fields are minimum, as expected, when it corresponds to the tilt of the bars ( $15^\circ$ ). When the mismatch of alignment between magnetic field and bars changes sign, the parallel electric field also does.

## PROSPECTS

This model constitutes the basis of the RF module of the future 3D full wave SSWICH code. RF sheaths physics would have to be included in the model as boundary conditions [10]. In a shorter timeframe, it can also be immediately used for coupling studies and producing field maps that can then be imported as input for the present version of SSWICH. Instead of importing a planar field map, a map of the parallel electric field on a contour of the antenna could be used. Nevertheless, repeating the procedure done in [1] and [11], we can substitute these field maps instead of TOPICA outputs. A relative comparison for AUG with the different antenna designs will be performed. The output of SSWICH could then be imported in EMC3-Eirene to simulate the new density distribution [12] and re-inject this new density into this model, thus closing the loop. Reproducing the variation of RF image currents with the strap power balance and phasing [13] would also be an interesting test. An accurate description of toroidal proximity effect due to the RF sheath voltages [14] and its link with the geometry would only be possible in 3D with appropriate boundary conditions.

## ACKNOWLEDGMENTS

This work has been carried out within the framework of the EUROfusion Consortium and has received funding from the Euratom research and training programme 2014-2018 under grant agreement No 633053. The views and opinions expressed herein do not necessarily reflect those of the European Commission.

## REFERENCES

- [1] J. Jacquot *Physics of Plasmas* **21**, 061509(11pp) (2014).
- [2] J.-P. Bérenger *J. Computational Physics* **114**, p185-200 (1994)
- [3] J. Jacquot *Plasma Physics Controlled Fusion* **55**, 115004(18pp) (2013).
- [4] F.L. Teixeira and W.C. Chew, *IEEE Microwave and Guided Wave Letters* **8**, p1804-1807 (1998)
- [5] A. Mendes, and et al., *Nuclear Fusion* **50**, 025021 (17pp) (2010).
- [6] L. Lu , *these proceedings* (2015).
- [7] V. Lancellotti, and et al., *Nuclear Fusion* **46**, S476S499 (2006).
- [8] L. Colas, and et al., *J. Nuclear Materials* **438**, S330S333 (2013).
- [9] V. Bobkov, and et al., *Nucl. Fusion* **53**, 093018 (9pp) (2013).
- [10] D. D'Ippolito, and J. Myra, *Physics of Plasmas* **13**, 102508 (12pp) (2006).
- [11] A. Křivská , *these proceedings* (2015).
- [12] W. Zhang, and et al., *these proceedings* (2015).
- [13] V. Bobkov, and et al., *these proceedings* (2015).
- [14] L. Colas , *these proceedings* (2015).